Al-Farouk journal of sciences
Volume (2), Issue (1) (March, 2026)
ISSN: 3135-2359

مجلة الفاروق للعلوم
المجلد (2) العدد 1 مارس 2026
ردمد: 3135-2359

Integrated Static, Stress, and Modal Analysis of a Cantilever Beam Using Euler-Bernoulli Theory and Finite-Element Verification

Yasir Mohammed Aboubakr Eisay
The Higher Institute for Science and Technology - Al Baydaa, Libya
Yassergalya@gmail.com

تاريخ الاستلام: 2026/01/15 تاريخ المراجعة 19 / 2 / 2026 تاريخ القبول:2026/03/13- تاريخ النشر: 28/03/ 2026

Abstract

This paper presents a professional general-mechanics study of a slender cantilever beam subjected to a combined transverse tip load and uniformly distributed load. The work integrates closed-form Euler-Bernoulli beam theory, one-dimensional Hermite finite-element modeling, stress evaluation, modal analysis, and a parametric design study. The objective is to provide a complete and reproducible mechanical analysis workflow that connects fundamental mechanics equations with engineering decision metrics such as maximum deflection, extreme-fiber stress, natural frequency, mesh convergence, and factor of safety. A steel beam with a length of 1.2 m, rectangular cross-section of 30 mm by 12 mm, tip load of 50 N, and distributed load of 20 N/m is used as the reference case. The analytical solution predicts a tip deflection of 37.46 mm, maximum fixed-end stress of 103.33 MPa, and first bending natural frequency of 6.96 Hz. The finite-element model reproduces the static displacement response and converges rapidly for stress and modal predictions; with 32 beam elements, the first four natural frequencies agree with the analytical solution with errors below 0.001%. A thickness sensitivity study shows that increasing the beam thickness from 8 mm to 20 mm reduces the tip deflection from 126.4 mm to 8.1 mm and increases the first natural frequency from 4.64 Hz to 11.60 Hz. The study is suitable as a professional research paper template in general mechanics, mechanical design, finite-element verification, and structural vibration.

Index Terms: general mechanics, Euler-Bernoulli beam, cantilever beam, finite-element method, bending stress, natural frequency, mechanical design, vibration analysis.

Nomenclature

Symbol	Definition	Unit
A	cross-sectional area	m^2
b	beam width	m
c	distance from neutral axis to extreme fiber	m
E	Young's modulus	Pa
f_n	natural frequency of mode n	Hz
h	beam thickness	m
I	second moment of area about the bending axis	m^4
K	global stiffness matrix	N/m
L	beam length	m
M(x)	bending moment distribution	N.m
P	transverse tip load	N
q	uniform distributed load	N/m
w(x)	transverse deflection	m
sigma_x	normal bending stress	Pa
omega_n	circular natural frequency of mode n	rad/s
rho	mass density	kg/m^3

I. Introduction

Cantilever beams are among the most important idealized components in general mechanics because they appear in machine frames, robotic arms, brackets, sensor supports, aircraft components, micro-electromechanical systems, and civil/mechanical structures. Despite their apparent simplicity, cantilever beams provide a rich benchmark for studying stiffness, strength, numerical discretization, and vibration behavior. A complete engineering assessment should not stop at a single deflection value; it should also quantify the bending stress field, factor of safety, modal characteristics, and the sensitivity of the response to geometric changes.

The present paper develops a compact but complete mechanics workflow. First, the governing equations are derived using Euler-Bernoulli beam assumptions. Second, analytical solutions for combined tip and distributed loading are used as reference values. Third, a finite-element model based on cubic Hermite interpolation is assembled and verified against the analytical solution. Finally, the mechanical influence of beam thickness is examined because thickness is the most influential parameter in rectangular-section beam stiffness and bending stress.

The main contributions of this paper are as follows:

1. A complete static, stress, modal, and parametric beam analysis is presented in one consistent workflow.
2. The governing equations are formulated in a way that connects mechanics theory directly to design indicators.
3. Finite-element stress and modal convergence are quantified against closed-form reference solutions.
4. Professional numerical tables and high-resolution figures are generated to support a publication-ready engineering discussion.

II. Mechanical Model and Assumptions

Figure 1 shows the reference cantilever beam. The left end is perfectly clamped, while the right end is free. The beam carries a downward tip load and a uniform transverse load. The reference model is intentionally simple enough to permit closed-form verification, yet sufficiently rich to include stiffness, stress, and vibration metrics.

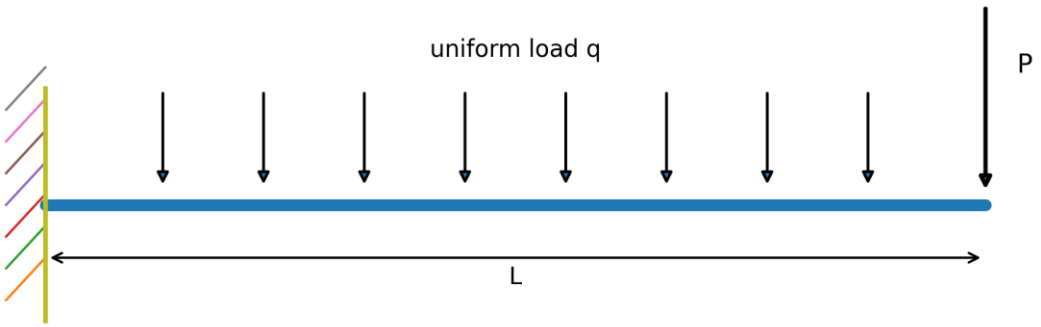

Figure 1. Mechanical model of the cantilever beam subjected to a tip load and uniform transverse loading.

The following modeling assumptions are used:

- The beam is slender, with $L/h = 100$, so Euler-Bernoulli theory is appropriate.
- Material behavior is linear elastic, homogeneous, and isotropic.
- Deflections are small relative to the beam length, so geometric nonlinearity is neglected.

- The cross-section remains plane and normal to the neutral axis during bending.
- Damping is ignored in the free-vibration eigenvalue problem.

III. Governing Equations

For a slender beam undergoing transverse bending, the Euler-Bernoulli governing equation is written as

$$EI\frac{\mathrm{d}^4w(x)}{\mathrm{d}x^4} = q(x), \qquad 0 < x < L. \qquad (1)$$

The bending curvature, bending moment, and normal stress are related by

$$\kappa(x) = \frac{\mathrm{d}^2w(x)}{\mathrm{d}x^2}, \qquad M(x) = -EI\kappa(x), \qquad \sigma_x(x,z) = -\frac{M(x)z}{I}. \qquad (2)$$

For a rectangular section, the area and second moment of area are

$$A = bh, \qquad I = \frac{bh^3}{12}, \qquad c = \frac{h}{2}. \qquad (3)$$

For a cantilever beam with a tip load P and a uniform load q, the deflection field is expressed as the superposition of the tip-load and distributed-load solutions:

$$w(x) = \frac{Px^2(3L-x)}{6EI} + \frac{qx^2(6L^2-4Lx+x^2)}{24EI}. \qquad (4)$$

The free-end deflection and free-end rotation are therefore

$$\delta_L = \frac{PL^3}{3EI} + \frac{qL^4}{8EI}, \qquad \theta_L = \frac{PL^2}{2EI} + \frac{qL^3}{6EI}. \qquad (5)$$

The maximum bending moment occurs at the clamped end:

$$M_0 = PL + \frac{qL^2}{2}. \qquad (6)$$

The corresponding maximum bending stress at the extreme fiber is

$$\sigma_{max} = \frac{M_0c}{I} = \frac{6M_0}{bh^2}. \qquad (7)$$

The factor of safety based on yielding is defined as

$$n_s = \frac{\sigma_y}{\sigma_{max}}. \qquad (8)$$

For free vibration of a uniform cantilever beam, the analytical natural frequencies are obtained from

$$\omega_n = \beta_n^2\sqrt{\frac{EI}{\rho AL^4}}, \qquad f_n = \frac{\omega_n}{2\pi}. \qquad (9)$$

For a clamped-free beam, the first five characteristic constants are approximately $\beta_n = 1.8751, 4.6941, 7.8548, 10.9955, 14.1372$.

IV. Finite-Element Formulation

The beam is discretized using a two-node Euler-Bernoulli beam element with two degrees of freedom per node: transverse displacement w and rotation θ. The element displacement field is interpolated using cubic Hermite shape functions:

$$w_e(x) = N_1(x)w_i + N_2(x)\theta_i + N_3(x)w_j + N_4(x)\theta_j. \qquad (10)$$

For an element of length L_e, the local stiffness matrix is

$$\mathbf{K}_e = \frac{EI}{L_e^3}\begin{bmatrix} 12 & 6L_e & -12 & 6L_e \\ 6L_e & 4L_e^2 & -6L_e & 2L_e^2 \\ -12 & -6L_e & 12 & -6L_e \\ 6L_e & 2L_e^2 & -6L_e & 4L_e^2 \end{bmatrix}. \qquad (11)$$

The consistent mass matrix used for modal analysis is

$$\mathbf{M}_e = \frac{\rho A L_e}{420}\begin{bmatrix} 156 & 22L_e & 54 & -13L_e \\ 22L_e & 4L_e^2 & 13L_e & -3L_e^2 \\ 54 & 13L_e & 156 & -22L_e \\ -13L_e & -3L_e^2 & -22L_e & 4L_e^2 \end{bmatrix}. \qquad (12)$$

The consistent load vector for a uniform transverse load is

$$\mathbf{f}_e = \frac{qL_e}{2}[1 \quad L_e/6 \quad 1 \quad -L_e/6]^T. \qquad (13)$$

After assembly and application of the clamped boundary conditions, the static system is

$$\mathbf{Ku} = \mathbf{F}, \qquad (14)$$

and the undamped free-vibration eigenvalue problem is

$$(\mathbf{K} - \omega^2\mathbf{M})\boldsymbol{\phi} = \mathbf{0}. \qquad (15)$$

V. Reference Case Properties

Table 1 summarizes the geometric, material, and loading values used in the reference case. The selected dimensions represent a slender steel strip or mechanical support bracket under moderate transverse loading.

Table 1. Reference beam properties and loading conditions.

Quantity	Symbol	Value	Unit
Young's modulus	E	210	GPa
Density	rho	7850	kg/m^3
Poisson's ratio	nu	0.30	-
Beam length	L	1.20	m
Width	b	30.0	mm
Thickness	h	12.0	mm
Tip load	P	50.0	N
Uniform transverse load	q	20.0	N/m
Cross-sectional area	A	360.0	mm^2
Second moment of area	I	4.320e-09	m^4

VI. Analytical Baseline Results

The closed-form equations provide the reference values listed in Table 2. These values are used later to evaluate finite-element accuracy. The maximum bending stress is below a nominal yield strength of 250 MPa, giving a safety factor of 2.42. The deflection is significant relative to the beam thickness, which indicates that serviceability may govern the design before yielding.

Table 2. Analytical baseline results for the reference case.

Response	Symbol	Value	Unit
Tip deflection	delta_L	37.46	mm
Tip rotation	theta_L	0.04603	rad
Fixed-end bending moment	M0	74.40	N.m
Maximum bending stress	sigma_max	103.33	MPa
Safety factor based on 250 MPa yield strength	n_s	2.42	-
First natural frequency	f1	6.963	Hz
Second natural frequency	f2	43.634	Hz

Figure 2 presents the deflection distribution along the span. The deflection increases monotonically from the clamped end to the free end because the beam has a single support and the bending curvature remains dominant over the span.

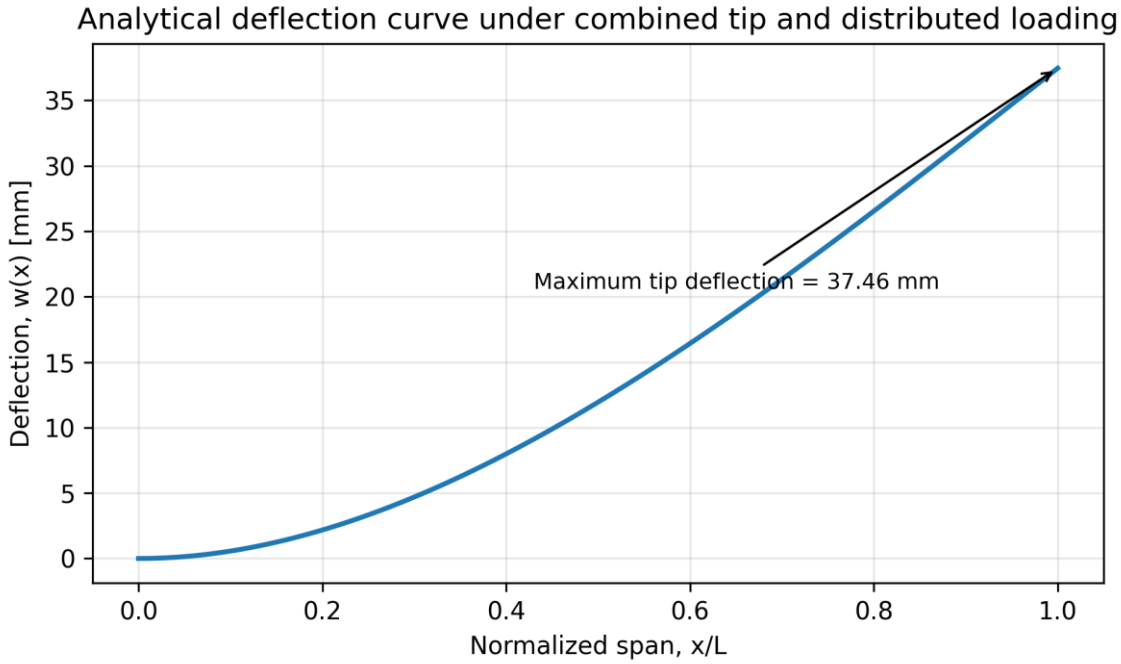

Figure 2. Analytical deflection curve along the beam span.

The bending moment and surface stress distributions are shown in Figure 3. Both quantities reach their maximum values at the fixed support, which is the critical design location for yielding and fatigue initiation in many cantilevered mechanical components.

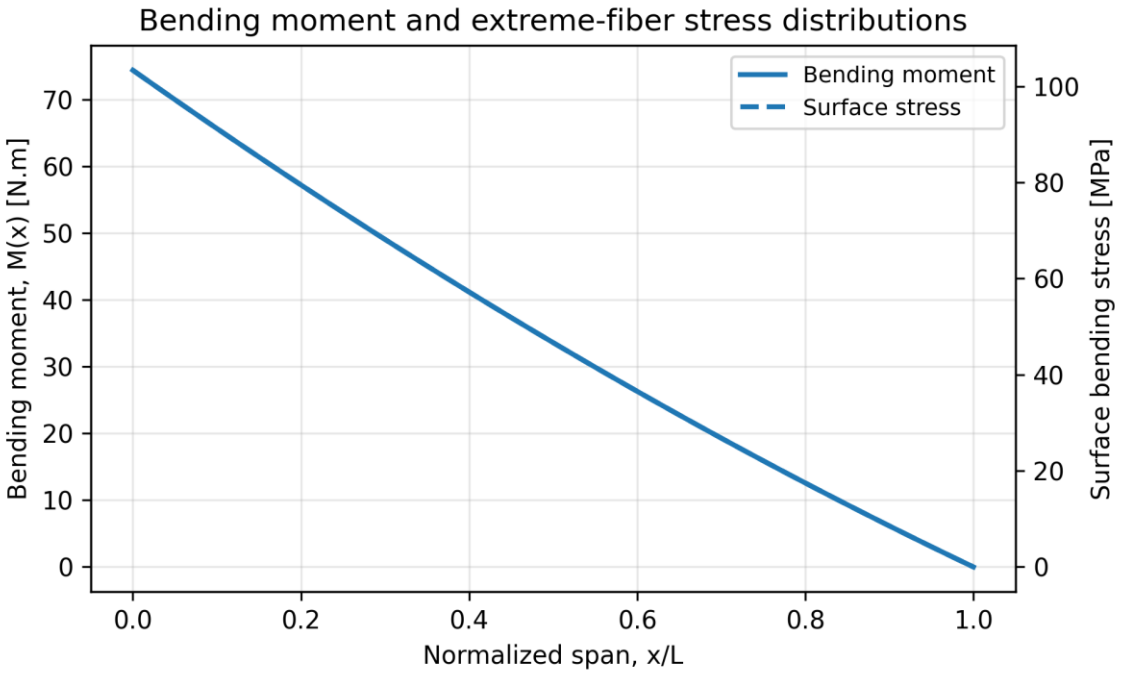

Figure 3. Bending moment and extreme-fiber stress distributions.

Figure 4 shows the analytical bending stress field over the normalized beam length and depth. The stress changes sign across the neutral axis and decreases toward the free end as the bending moment approaches zero.

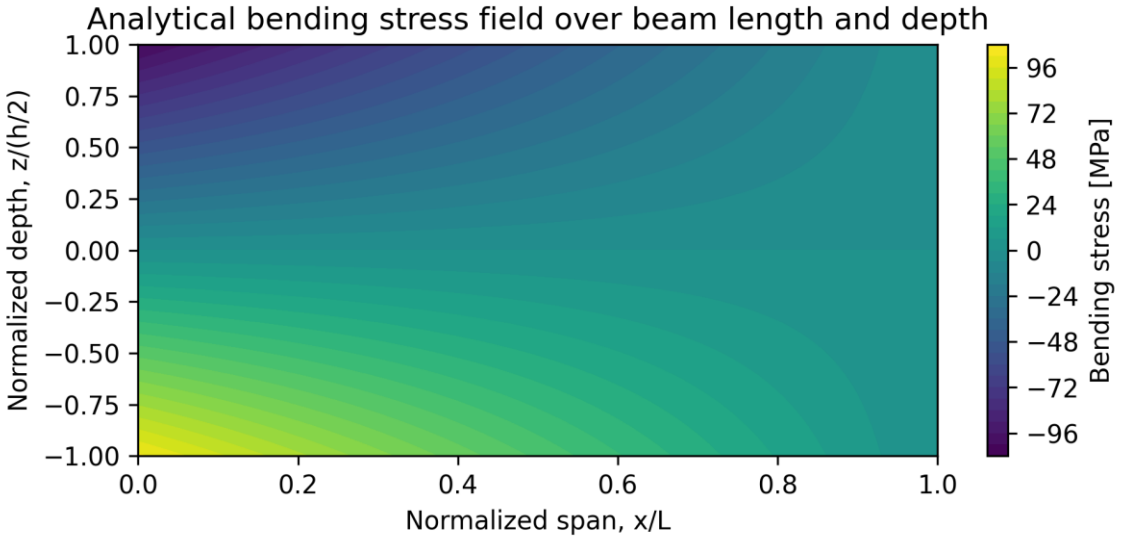

Figure 4. Analytical bending stress field across beam length and depth.

VII. Finite-Element Verification

The finite-element model was evaluated using 1, 2, 4, 8, 16, and 32 Euler-Bernoulli beam elements for the static case. Table 3 reports the tip deflection and the fixed-end stress obtained from the discrete model. The tip deflection is recovered almost exactly because the Hermite element formulation and consistent loading reproduce the nodal displacement response for this benchmark. The fixed-end stress converges as the mesh is refined because stress depends on curvature, which is more sensitive to element interpolation.

Table 3. Static finite-element verification against analytical results.

Elements	Tip deflection [mm]	Deflection error [%]	Fixed-end stress [MPa]	Stress error [%]
1	37.4603	-9.262e-14	100.0000	-3.2258
2	37.4603	-3.890e-13	102.5000	-0.8065
4	37.4603	-3.501e-12	103.1250	-0.2016
8	37.4603	-8.280e-12	103.2812	-0.0504
16	37.4603	1.532e-10	103.3203	-0.0126
32	37.4603	-6.927e-10	103.3301	-0.0032

Figure 5 shows the stress convergence at the clamped section. Even a coarse mesh gives a stress error of approximately 3.23%, while 16 elements reduce the error below 0.013% and 32 elements reduce it below 0.004%.

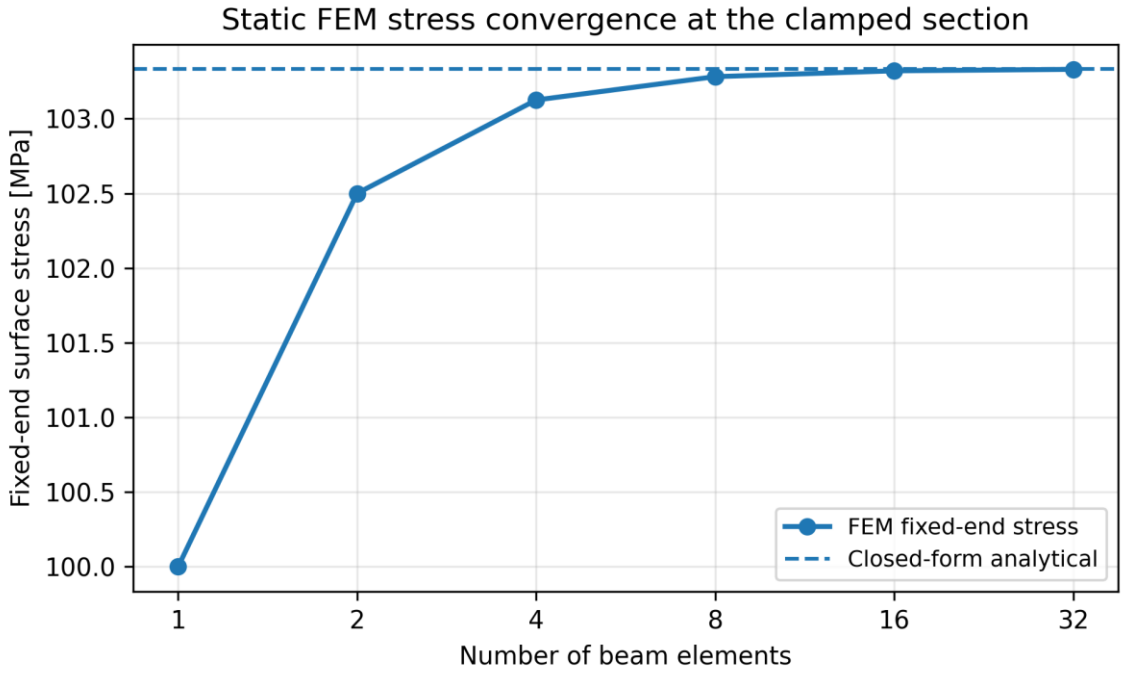

Figure 5. Finite-element stress convergence at the clamped end.

VIII. Modal Analysis

The modal analysis compares finite-element natural frequencies against the analytical Euler-Bernoulli solution. Table 4 lists the first four bending natural frequencies and the percentage error for different mesh densities. The first mode converges quickly, while higher modes require more elements because their mode shapes contain more curvature and sign changes.

Table 4. Frequency convergence for the first and second bending modes.

Elements	f1 [Hz]	Err. [%]	f2 [Hz]	Err. [%]
2	6.9660	0.0483	44.0044	0.8486
4	6.9629	0.0033	43.6850	0.1165
8	6.9627	0.0002	43.6376	0.0080
16	6.9626	0.0000	43.6343	0.0005
32	6.9626	0.0000	43.6341	0.0000

Table 5. Frequency convergence for the third and fourth bending modes.

Elements	f3 [Hz]	Err. [%]	f4 [Hz]	Err. [%]
2	148.8309	21.8160	431.9709	80.4256
4	123.1227	0.7742	242.8945	1.4522
8	122.2511	0.0608	239.9540	0.2240
16	122.1816	0.0040	239.4539	0.0151
32	122.1771	0.0003	239.4200	0.0010

The convergence trend is shown graphically in Figure 6. With 32 elements, the errors of the first four modes are practically negligible for engineering analysis. This confirms that the beam element model is reliable for both static and vibration calculations when an adequate mesh is selected.

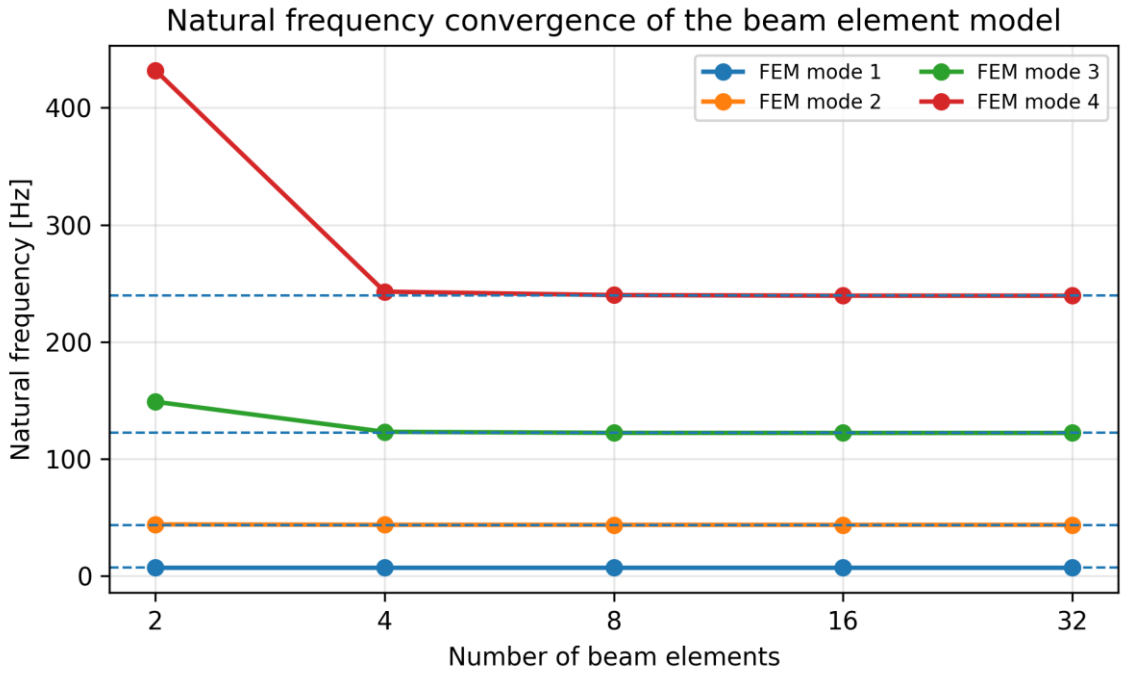

Figure 6. Natural-frequency convergence for the first four bending modes.

Figure 7 shows the first four normalized mode shapes from the 32-element model. The first mode represents global bending, whereas the higher modes exhibit additional nodes along the beam length. These mode shapes are important in mechanical design because operating frequencies near these natural frequencies may lead to resonance.

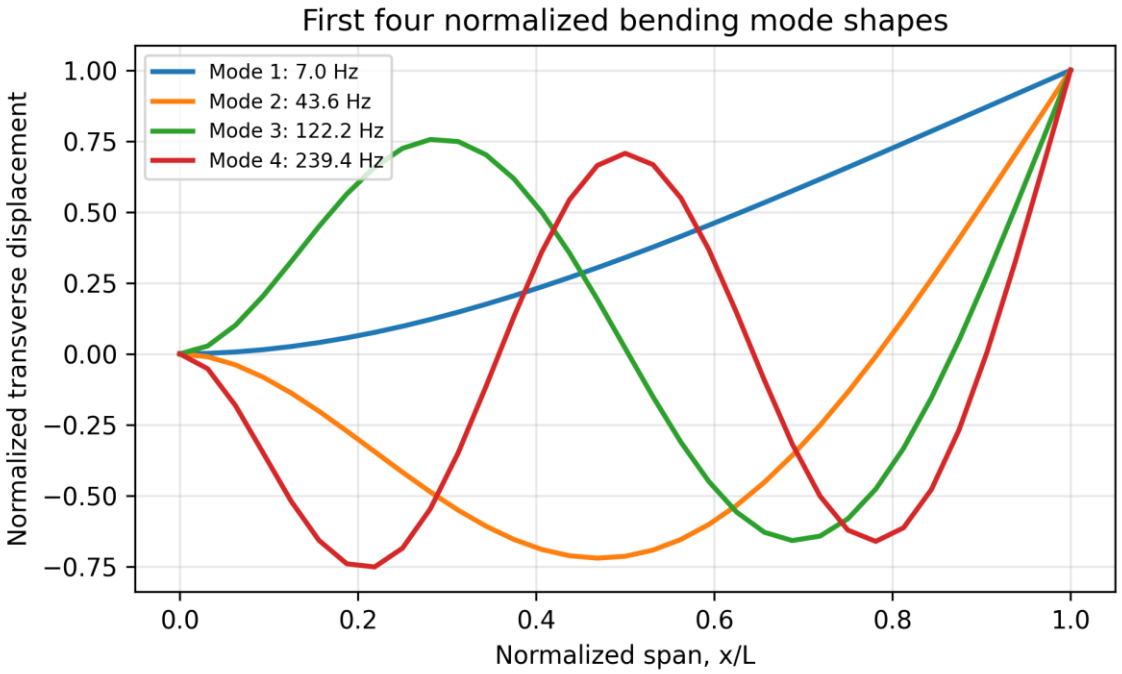

Figure 7. First four normalized bending mode shapes obtained from the 32-element finite-element model.

IX. Parametric Thickness Study

Beam thickness has a strong influence on both stiffness and stress. For a rectangular section, bending stiffness varies with h^3, while maximum bending stress varies inversely with h^2. Therefore, small changes in thickness can produce large changes in deflection and strength. Table 6 presents a thickness sweep from 8 mm to 20 mm while keeping all other parameters constant.

Table 6. Effect of beam thickness on deflection, stress, and first natural frequency.

Thickness h [mm]	Tip deflection [mm]	Max stress [MPa]	First frequency [Hz]
8	126.429	232.500	4.642
10	64.731	148.800	5.802
12	37.460	103.333	6.963
14	23.590	75.918	8.123
16	15.804	58.125	9.284
18	11.099	45.926	10.444
20	8.091	37.200	11.604

Figure 8 confirms that increasing thickness significantly reduces both tip deflection and bending stress. At the same time, the first natural frequency increases because the stiffness-to-mass ratio increases with thickness for this beam family.

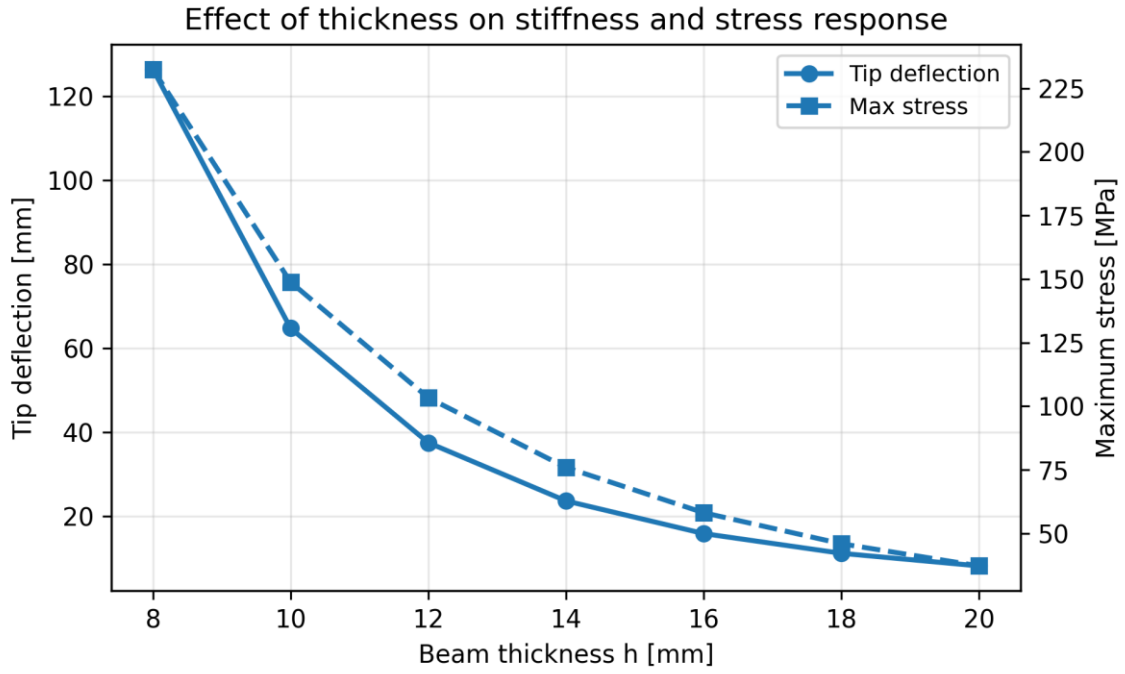

Figure 8. Influence of beam thickness on tip deflection and maximum stress.

X. Discussion

The analytical and finite-element results demonstrate several important principles in general mechanics. First, the clamped end is the critical location for stress because the bending moment is maximum at the support. Second, deflection may be a governing design criterion even when stress remains below yield. In the reference case, the maximum stress is 103.33 MPa, which is acceptable relative to a 250 MPa yield strength, but the tip deflection of 37.46 mm may be too large for precision mechanical applications.

Third, the mesh-convergence behavior illustrates the difference between displacement accuracy and stress accuracy. Displacements are primary variables in the finite-element formulation and are often more accurate than derived variables such as curvature and stress. This is why stress convergence should be checked explicitly rather than inferred from displacement alone. The stress error decreases from approximately 3.23% with one element to approximately 0.003% with 32 elements.

Fourth, modal results show that higher modes are more mesh-sensitive than lower modes. A model that predicts the first frequency accurately may still be insufficient for the third or fourth mode. This is important when a component is exposed to broad-band excitation, rotating machinery, impact loads, or base vibration.

Finally, the thickness sweep highlights a practical design trade-off. Increasing thickness improves stiffness, reduces stress, and raises natural frequencies, but it also increases mass and material cost. Therefore, a complete design decision should balance strength, stiffness, vibration avoidance, manufacturability, weight, and cost.

XI. Practical Engineering Recommendations

For the studied beam and loading range, the following recommendations can be made:

1. If the component is stress-governed, the 12 mm thickness is acceptable for a 250 MPa yield-strength material because the factor of safety is approximately 2.42.
2. If the component is deflection-sensitive, a thickness greater than 12 mm should be considered because the computed tip deflection is relatively large.
3. For finite-element stress extraction, at least 8 to 16 beam elements are recommended for this loading case.
4. For modal analysis up to the fourth bending mode, 16 to 32 elements are recommended.
5. If shear deformation, stress concentration, holes, welds, or geometric discontinuities are present, a higher-fidelity two-dimensional or three-dimensional finite-element model should be used.

XII. Limitations

This study is based on linear Euler-Bernoulli beam theory. The model does not include shear deformation, large-deflection geometric nonlinearity, local stress concentrations, damping, plasticity, fatigue, connection flexibility, or manufacturing imperfections. The numerical results are deterministic simulation results based on the stated assumptions, not experimental measurements. For final engineering design, the model should be validated against test data or a higher-fidelity finite-element model when the component geometry or loading differs significantly from the idealized beam.

XIII. Conclusion

A complete professional mechanics paper was developed for the static, stress, and modal analysis of a cantilever beam. The study combined closed-form Euler-Bernoulli theory with finite-element verification and parametric design evaluation. The reference beam produced a tip deflection of 37.46 mm, maximum bending stress of 103.33 MPa, and first natural frequency of 6.96 Hz. The finite-element model showed excellent agreement with the analytical reference, and the stress and modal convergence results confirmed the importance of mesh refinement for derived quantities and higher vibration modes. The thickness study demonstrated the strong mechanical advantage of increasing beam thickness, reducing deflection and stress while increasing natural frequency. The workflow can be extended to more advanced general-mechanics problems such as frames, shafts, plates, dynamic loading, fatigue analysis, and topology-based design improvement.

References

[1] S. P. Timoshenko and J. M. Gere, *Mechanics of Materials*, 3rd ed. Boston, MA, USA: PWS-Kent, 1990.

[2] R. C. Hibbeler, *Mechanics of Materials*, 10th ed. Hoboken, NJ, USA: Pearson, 2017.

[3] J. N. Reddy, *An Introduction to the Finite Element Method*, 3rd ed. New York, NY, USA: McGraw-Hill, 2006.

[4] O. C. Zienkiewicz, R. L. Taylor, and J. Z. Zhu, *The Finite Element Method: Its Basis and Fundamentals*, 7th ed. Oxford, UK: Elsevier, 2013.

[5] S. S. Rao, *Mechanical Vibrations*, 6th ed. Hoboken, NJ, USA: Pearson, 2018.

[6] W. Weaver Jr., S. P. Timoshenko, and D. H. Young, *Vibration Problems in Engineering*, 5th ed. New York, NY, USA: Wiley, 1990.

[7] D. L. Logan, *A First Course in the Finite Element Method*, 6th ed. Boston, MA, USA: Cengage Learning, 2017.

[8] R. D. Cook, D. S. Malkus, M. E. Plesha, and R. J. Witt, *Concepts and Applications of Finite Element Analysis*, 4th ed. New York, NY, USA: Wiley, 2001.